

# UC Irvine

## UC Irvine Previously Published Works

### Title

Intrathecal infusion of BMAA induces selective motor neuron damage and astrogliosis in the ventral horn of the spinal cord.

### Permalink

<https://escholarship.org/uc/item/8qq8t80f>

### Authors

Yin, Hong  
Yu, Stephen  
Hsu, Cheng-I  
[et al.](#)

### Publication Date

2014-11-01

### DOI

10.1016/j.expneurol.2014.06.003

Peer reviewed

Published in final edited form as:

*Exp Neurol.* 2014 November ; 0: 1–9. doi:10.1016/j.expneurol.2014.06.003.

## Intrathecal infusion of BMAA induces selective motor neuron damage and astrogliosis in the ventral horn of the spinal cord

Hong Z. Yin, MD<sup>a</sup>, Stephen Yu<sup>a</sup>, Cheng-I Hsu, PhD<sup>a</sup>, Joe Liu<sup>a</sup>, Allan Acab<sup>a</sup>, Richard Wu<sup>a</sup>, Anna Tao<sup>a</sup>, Benjamin J. Chiang<sup>a</sup>, and John H. Weiss, MD, PhD<sup>a,b,\*</sup>

<sup>a</sup>Department of Neurology, University of California, Irvine, USA

<sup>b</sup>Department of Anatomy & Neurobiology, University of California, Irvine, USA

### Abstract

The neurotoxin beta-N-methylamino-L-alanine (BMAA) was first identified as a “toxin of interest” in regard to the amyotrophic lateral sclerosis–Parkinsonism Dementia Complex of Guam (ALS/PDC); studies in recent years highlighting widespread environmental sources of BMAA exposure and providing new clues to toxic mechanisms have suggested possible relevance to sporadic ALS as well. However, despite clear evidence of uptake into tissues and a range of toxic effects in cells and animals, an animal model in which BMAA induces a neurodegenerative picture resembling ALS is lacking, possibly in part reflecting limited understanding of critical factors pertaining to its absorption, biodistribution and metabolism. To bypass some of these issues and ensure delivery to a key site of disease pathology, we examined effects of prolonged (30 day) intrathecal infusion in wild type (WT) rats, and rats harboring the familial ALS associated G93A SOD1 mutation, over an age range (80±2 to 110±2 days) during which the G93A rats are developing disease pathology yet remain asymptomatic. The BMAA exposures induced changes that in many ways resembles those seen in the G93A rats, with degenerative changes in ventral horn motor neurons (MNs) with relatively little dorsal horn pathology, marked ventral horn astrogliosis and increased 3-nitrotyrosine labeling in and surrounding MNs, a loss of labeling for the astrocytic glutamate transporter, GLT-1, surrounding MNs, and mild accumulation and aggregation of TDP-43 in the cytosol of some injured and degenerating MNs. Thus, prolonged intrathecal infusion of BMAA can reproduce a picture in spinal cord incorporating many of the pathological hallmarks of diverse forms of human ALS, including substantial restriction of overt pathological changes to the ventral horn, consistent with the possibility that environmental BMAA exposure could be a risk factor and/or contributor to some human disease.

© 2014 Elsevier Inc. All rights reserved.

\*Address correspondence to: 2101 Gillespie Building Department of Neurology, University of California, Irvine Irvine, CA 92697-4292 Tel: (949) 824-6774 Fax: (949) 824-1668 jweiss@uci.edu.

**Publisher's Disclaimer:** This is a PDF file of an unedited manuscript that has been accepted for publication. As a service to our customers we are providing this early version of the manuscript. The manuscript will undergo copyediting, typesetting, and review of the resulting proof before it is published in its final citable form. Please note that during the production process errors may be discovered which could affect the content, and all legal disclaimers that apply to the journal pertain.

## Keywords

BMAA; beta-N-methylamino-L-alanine; neurotoxin; ALS; amyotrophic lateral sclerosis; motor neuron; G93A rat; SOD1; animal model

---

## Introduction

Amyotrophic lateral sclerosis (ALS) is an adult onset neurodegenerative disease characterized by the selective loss of upper and lower motor neurons (MNs). A rare form of the disease called Guam ALS– Parkinsonism Dementia Complex (ALS/PDC) comprises ALS, often with associated symptoms of Parkinsonism and Alzheimer’s like dementia, occurred in native Chamorro populations with an incidence >50 times that of ALS in most of the world (Arnold et al., 1953; Koerner, 1952; Mulder et al., 1954). Intensive epidemiological studies implicated environmental exposures (Garruto and Yase, 1986; Spencer, 1987), with early attention focusing on highly toxic cycad seeds, which were used for food after repetitive washing and cooking (Kurland, 1972; Whiting, 1963), and a neurotoxic non-protein amino acid, beta-N-methylamino-L-alanine (BMAA, also known as alpha-amino-beta-methylaminopropanoic acid) which they contained (Vega and Bell, 1967). Large oral doses of BMAA were reported to induce a syndrome in primates with features of ALS (Spencer et al., 1987), but the apparent low potency of BMAA and low levels found in washed cycad flour compared to amounts used in the study led to doubts to its relevance to human disease (Duncan et al., 1990).

Findings over the past decade have highlighted new sources for BMAA exposure and led to a resurgence of the BMAA hypothesis. It is now apparent that BMAA is produced by diverse taxa of cyanobacteria found worldwide (Cox et al., 2005; Metcalf et al., 2008), that BMAA appears to be either tightly associated with or incorporated into proteins of organisms that have been exposed to it, where it may reside for prolonged periods of time and be released by hydrolysis (Murch et al., 2004a), and that BMAA may be present in human tissues not only of Chamorros who died of Guam ALS/PDC but in tissues from sporadic ALS and Alzheimer’s patients in North America and other regions (Murch et al., 2004b; Pablo et al., 2009). This, together with findings of high levels of protein associated BMAA in washed cycad flour as well as in food species present in aqueous environments prone to cyanobacterial blooms suggests that BMAA exposures outside of Guam may be far more widespread than previously believed (Bradley et al., 2013; Brand et al., 2010; Jonasson et al., 2010; Murch et al., 2004a). Indeed, consistent with the apparent close protein association of BMAA, it appears that BMAA does bioaccumulate, with long-lasting residence in tissues and increasing levels often found at higher trophic levels of the food chain (Brand et al., 2010; Cox et al., 2003; Jonasson et al., 2010; Mondo et al., 2012). However, although BMAA is clearly neurotoxic with diverse effects in different model systems, an animal model reproducing key pathological features of ALS via systemic administration has been lacking (Karamyan and Speth, 2008).

In prior studies of BMAA toxicity to spinal cord neurons in culture, we found that BMAA was weakly toxic to most spinal neurons, but induced MN injury with far greater potency

(Rao et al., 2006). Thus, the primary aim of the present study was to examine effects of prolonged BMAA exposure *in vivo*, to see if it could reproduce a more complete picture of ALS-like spinal cord pathology incorporating distinctive changes in other cell types, including astrocytes as well as in MNs themselves. In order to bypass variables and unknowns related to absorption, distribution and metabolism of BMAA *in vivo*, we opted to examine effects of direct delivery to the spinal cord, carrying out prolonged (30 day) intrathecal infusion of this toxin in both wild type rats, and in rats overexpressing the familial ALS associated G93A SOD1 mutation. We find that BMAA exposure induced changes in ventral horn MNs and in nearby astrocytes that were remarkably reminiscent of changes seen in untreated rats harboring the familial ALS associate G93A mutation in the Cu/Zn superoxide dismutase gene (SOD1), with manifestations in both models substantially localized to the ventral horn region of the spinal cord (where MNs reside), and markedly fewer changes noted in dorsal horn. Present studies thus indicate that with direct application, BMAA is capable of inducing spinal cord degenerative changes with similarities to those seen in both SOD1 linked animal models and human ALS, and are consistent with the hypothesis that BMAA is a contributory factor to some human ALS.

## Materials and methods

### Animals

Male hemizygous SOD1 G93A transgenic rats [Tac:N:(SD)-TgN(SOD1G93A)L26H, obtained from the Emerging Models Program sponsored by Amyotrophic Lateral Sclerosis Association, Taconic laboratories, Germantown, NY] were bred with wild-type females, and offspring genotyped by PCR analysis (Howland et al., 2002); wild-type siblings serve as controls for mutant animals. Animals are killed when they can no longer right themselves within 10 s of being pushed on their side. All animal procedures were approved by the Institutional Animal Care and Use Committee.

### Surgical procedures

Intrathecal infusion studies used rats at 80±2 days of age (body weight 250g-380g). Anesthesia was induced using 5% isoflurane, and maintained at 2.5% at a flow rate of 1 l/min. Catheter and reservoir placement were carried out largely as previously described (Yin et al., 2007). Briefly, an incision was made in the dorsal head and the atlanto-occipital membrane, through which a PE5 catheter was inserted into the subarachnoid space and advanced 7–10 cm to the lumbar enlargement. The catheter was connected to an Alzet mini-osmotic pump model 2004; 200 µl volume, 0.25 µl/h × 30 days) which was pre-filled with 5mM BMAA or saline. After surgery, animals were housed individually and body weight recorded daily. In addition, evidence of pain or infection and motor dysfunction were closely monitored. Animals were sacrificed if they appeared distressed or if after 5 days, motor function remained impaired or body weight had not recovered to pre-surgery levels.

### Tissue preparation and staining

Thirty days after the start of intrathecal infusions, the animals were anesthetized with isoflurane, and perfused transcardially with saline, followed by 4% paraformaldehyde (PFA) for 10 min. The lumbar enlargements of spinal cords were dissected and post-fixed in 4%

PFA for 24 h and removed to 30% sucrose/PBS for another 2 days. Serial 20- $\mu$ m frozen sections were cut from the middle of the lumbar enlargement for ~ 5 mm in the caudal direction.

After every 10 sections, 3–5 serial sections were set aside for staining.

Immunohistochemical stains were carried out on floating sections, blocked (10% HS, 1 h), and exposed to primary antibody in 10% HS, 0.3% Triton-X 100 (SMI-32, 1:8000 IP, Sternberger Monoclonals, Berkeley, CA; GLT-1, 1:1000 IF, Chemicon, Temecula, CA; 3-nitrotyrosine, 10  $\mu$ g/ml IF, Upstate Biotechnology, Waltham, MA; TDP-43, 1:10,000 IP, Proteintech Group, Chicago, IL). Labeling was visualized either by routine ABC immunoperoxidase techniques or under fluorescence using secondary antibodies linked to fluorophores (Alexafluor 488, Molecular Probes, Eugene, OR).

### Quantification of histopathological changes

Surviving MNs were counted in ventral horn of lumbar spinal slices from each condition. MNs displaying pyknotic nuclei, marked atrophy or swelling, or fragmentation of the proximal dendrites were not counted as alive (Fig. 2).

For examination of 3-NT and GLT-1 labeling staining in the neuropil surrounding ventral horn MNs, care was taken to ensure that all slices from each experiment were labeled using identical simultaneous antibody exposures, and fluorescence photographs taken with identical camera settings so that labeling intensities could be compared. For quantification of GLT-1 labeling, photographs were imported into an image analysis package (Image J, public domain software from the NIH) as 8-bit gray scale images, and two regions were marked around each readily identifiable MN: one precisely outlining the circumference of the MN and another 10  $\mu$ m further out (with any other neurons or neuronal processes masked out). The space between these regions was defined as the *surround zone*. After subtraction of background fluorescence, averaged intensity was calculated within each surround zone.

### Chemicals and reagents

BMAA was obtained from Sigma (St. Louis, MO). Antibodies were from the following sources: SMI-32, Sternberger Monoclonals, Berkeley, CA; GLT-1, Chemicon, Temecula, CA; 3-nitrotyrosine, Upstate Biotechnology, Waltham, MA; TDP-43, Proteintech Group, Chicago, IL. For fluorescence labeling, we used secondary antibodies linked to Alexafluor 488 (Molecular Probes, Eugene, OR). All other chemicals and reagents were obtained from common commercial sources.

## Results

### Intrathecal infusion of BMAA causes preferential MN injury

We set out to undertake a four-way comparison, examining pathological features of the lumbar spinal cord in wild type rats infused with saline only (WT+saline), or with BMAA (WT+BMAA), with features in age matched sibling G93A SOD1 transgenic rats infused with saline only (Tg+saline) or with BMAA (Tg+BMAA). In choosing the age for the study animals, we desired the SOD1 mutant animals to be pre-symptomatic, yet old enough that

early pathological changes are evident. As these animals generally showed initial symptoms at ~ 140-160 days of age, we chose to start the intrathecal infusions at an age of  $80\pm 2$  days, when early pathological changes are apparent (Howland et al., 2002; Yin et al., 2007), with sacrifice for histological analysis 30 days later ( $110\pm 2$  days). Catheters, connected to Alzet osmotic minipumps loaded with either saline alone or with 5 mM BMAA, were inserted in the cervical spine, and threaded intrathecally to terminate in the region of the lumbar enlargement as previously described (Yin et al., 2007) (see Materials and Methods).

MN degeneration was assessed in lumbar spinal cord sections with Nissl stain, and immunocytochemically using an antibody to non-phospholated neurofilament epitopes, SMI-32, which strongly labels MNs as well as their neuritic processes (Carriedo et al., 1996; Rao et al., 2006). In the WT+saline condition virtually all MNs appeared healthy. However, in the transgenics (Tg+saline), there were many MNs in differing stages of degeneration, manifested by a spectrum of changes including cellular and nuclear constriction, eccentric nuclei, swelling, vacuolar changes and fragmentation of processes. Many degenerating MNs were surrounded by microglia, with some appearing to be fully replaced by glial nodules and (Figs. 1, 2). In The WT+BMAA condition, a similar spectrum and frequency of MN degenerative changes was seen, with some MNs showing atrophic changes and some showing more swelling with evident vacuolar changes. In addition, microglial infiltration and some microglial nodules were noted in this condition as well.

One question we were eager to address was whether BMAA infusion into the mutant SOD1 rat spinal cords (Tg+BMAA) would elicit synergistic injury. Leading us to consider it likely that we would see synergism, BMAA can induce neuronal injury via excitotoxic activation of glutamate receptors (Chiu et al., 2011; Vyas and Weiss, 2009), and mutant SOD1 has been reported to increase susceptibility to excitotoxic injury in both dissociated culture (Roy et al., 1998), and spinal cord slice culture (Yin and Weiss, 2012) models. However, in the present paradigm, we did not observe evidence of marked synergism, with evident MN degeneration in the Tg+BMAA condition not substantially different from that observed in WT+BMAA or Tg+saline conditions (Fig. 2).

A further pathological hallmark of MNs seen in most ALS cases is the presence of cytosolic protein inclusions. To assess possible cytosolic protein aggregation, we carried out immunostains for the peptide, TDP-43, which is normally present in the nucleus, where it has roles in RNA processing, and has been observed to leave the nucleus and to accumulate in cytosolic aggregates in diseased MNs in diverse forms of human ALS (Neumann et al., 2006). Interestingly, whereas such distinctive TDP-43 pathology is not a prominent early feature of rodent SOD1 mutant ALS models (Robertson et al., 2007; Turner et al., 2008), it has been observed in damaged MNs in these animals at advanced stages of the disease (Shan et al., 2009). For these studies, we used an antibody against the N-terminal region of TDP-43, expression of which is normally quite strongly restricted to the nucleus, as we found to be the case in virtually all MNs in the WT+saline condition. However, loss of distinct nuclear TDP-43 labeling with appearance of some cytosolic staining was noted in a fraction of the damaged and degenerating MNs in the other three conditions, with little difference noted in either the frequency or appearance of cytosolic TDP-43 labeling between them (Fig. 3).

## Pathological changes in astrocytes

Immunostains employing three different antibodies were undertaken to examine distinct aspects of astrocyte pathology. First, reactive astrogliosis was assessed using the astrocyte marker, glial fibrillary acidic protein (GFAP). Ventral horn astrogliosis is a prominent feature of human ALS, and progressive astrogliosis occurs prominently in SOD1 mutant rodent models of ALS, including the G93A rat model examined in these studies (Howland et al., 2002; Yin et al., 2007). Notably, astrocyte pathology in both human disease and the SOD1 mutant rodent models is highly restricted, with prominent changes in the ventral horn astrocytes which are adjacent to disease affected MNs, with a paucity of changes in dorsal horn astrocytes until late stages of the disease.

In the control (WT+saline) condition, most GFAP labeled astrocytes in the ventral horn were small and faintly labeled. In contrast, WT+BMAA, Tg+saline, and Tg+BMAA conditions each showed substantial increases in both numbers of labeled astrocytes as well as in their size and intensity of labeling in ventral horn. Interestingly, dorsal horn astrocytes appeared little different from control in the WT+BMAA and Tg+saline conditions, but, although not quite statistically significant over the set of 5-8 animals studied, appeared in most animals to be modestly increased in both number and labeling intensity in the Tg +BMAA condition, possibly compatible with some degree of synergism between effects of the SOD1 mutation and the BMAA that is not readily evident under the present exposure paradigm (Fig. 4).

Oxidative tissue damage, and particularly increases in labeling for the oxidative damage marker, 3-nitrotyrosine (3-NT), occurs in both human and SOD1 mutant rodent models of ALS (Beal et al., 1997; Ferrante et al., 1997; Yin et al., 2007). Immunolabeling for 3-NT reveals increased labeling in the ventral horn compared to surrounding white matter pathways, which is evident even in the WT+saline condition. Although we and other have previously found strong increases in ventral horn 3-NT labeling in late presymptomatic G93A SOD1 mutant rats compared to WT rats, we observed relatively little difference between the WT+saline and Tg+saline conditions here, likely reflecting the age of the animals compared to the time of disease onset (~110 days, with symptoms appearing at ~140-165 days). However, the presence of BMAA (in both WT+BMAA and Tg+BMAA conditions) resulted in a marked increase in ventral horn 3-NT labeling, which, much as we have previously described in the presymptomatic G93A mutant animals (Rao and Weiss, 2004; Rao et al., 2003; Yin et al., 2007), was particularly evident in the neuropil surrounding and between MNs (Fig. 5), consistent with the idea that MN dysfunction contributes directly to the 3-NT labeling in adjacent astrocytes.

The third marker of astrocyte pathology we examined was the astrocytic glutamate transporter, GLT-1. Loss of astrocytic glutamate transport capacity, resulting specifically from loss or dysfunction of the GLT-1 transporter, is seen in human ALS (Rothstein et al., 1992; Rothstein et al., 1995), a finding that lent initial strong support to the idea that excitotoxic activation of glutamate receptors might contribute to MN damage in the disease. Furthermore, loss of GLT-1 occurs prominently in the G93A rats employed in this study (Howland et al., 2002; Yin et al., 2007). As has been previously noted, labeling of control slices for the astrocytic glutamate transporter, GLT-1, shows diffuse staining throughout the

spinal cord gray matter. However, a rim of particularly strong labeling is often seen immediately surrounding MN somata, which we have previously found be markedly decreased even in presymptomatic SOD1 mutant rats (Yin et al., 2007). To quantify these changes, we measured the intensity of GLT-1 labeling in 10  $\mu\text{m}$  zones surrounding identified MNs in the spinal cord slices as described (see Materials and Methods). We found that BMAA induced significant decreases in the intensity of GLT-1 labeling in the surround zones that was nearly as great as those induced in the Tg+saline and Tg+BMAA conditions (Fig. 6).

## Discussion

### Summary of principal findings

We find that 30 day intrathecal infusions of BMAA induce a distinctive pathological picture in the spinal cord, which shows striking similarities to that seen in rats harboring the G93A SOD1 mutation. Notably, despite being an exogenously applied toxin, which should have equal access to ventral horn and dorsal horn tissues within the spinal cord, the pathological changes induced by BMAA infusions were reminiscent of those seen in the mutant SOD1 rats, with a strong preponderance of changes seen in the ventral horn region, where the MNs reside. Interestingly, BMAA and mutant SOD1 each induced a similar spectrum of pathological changes among the MNs, including some MNs demonstrating swelling and vacuolar changes, while others showed prominent atrophic changes, and some were surrounded by microglia or replaced by microglial nodules. In addition, as noted in the SOD1 mutant rats, the BMAA infusion resulted in loss of nuclear TDP-43 labeling with speckled accumulation in cytosol of some of the damaged and degenerating MNs.

Distinctive changes resembling those in the SOD1 mutant rats were also noted in the astrocytes and neuropil surrounding damaged ventral horn MNs, with prominent astrogliosis, as well as increases in 3-NT labeling, and a loss of GLT-1 from the region immediately surrounding MNs. Surprisingly, in the present paradigm, we noted relatively little synergism between the effects of BMAA and of the G93A mutation, with ventral horn changes induced by BMAA infusion in G93A mutant rats little different from those caused by either alone. The only suggestion of synergism was in the case of GFAP staining in the dorsal horn, where, although not reaching statistical significance, in most animals numbers of GFAP labeled astrocytes was modestly greater in the Tg+BMAA condition. The reasons for the paucity of apparent synergism is uncertain, but perhaps synergistic effects would become more evident either pathologically or clinically with greater durations of co-exposure.

### Clues to mechanisms of MN vulnerability in ALS

Despite a large number of studies and numerous clues, the basis of the selective vulnerability of MNs in ALS is poorly understood. As discussed above, findings of loss of astrocytic glutamate transport in ALS supported an “excitotoxic” contribution (Rothstein et al., 1992). Glutamate activates distinct families of ionotropic receptors, including the highly  $\text{Ca}^{2+}$  permeable NMDA receptors and the generally  $\text{Ca}^{2+}$  impermeable AMPA and kainate receptors. Whereas most studies of excitotoxic neurodegeneration have thus focused on



contributions of NMDA receptors, some AMPA receptors gate channels that are directly permeable to  $\text{Ca}^{2+}$  (“Ca-AMPA receptors”), reflecting absence of the GluA2 (formerly called GluR2) subunit in heteromeric channels. MNs possess large numbers of these unusual Ca-AMPA receptors, making them highly sensitive to AMPA receptor mediated injury (Carriedo et al., 1995; Carriedo et al., 1996; Van Den Bosch et al., 2000; Vandenberghe et al., 2000). Another factor that may contribute to MN vulnerability is that they have low levels of cytosolic  $\text{Ca}^{2+}$  binding proteins (Alexianu et al., 1994; Elliott and Snider, 1995), causing them to buffer cytosolic  $\text{Ca}^{2+}$  poorly (Lips and Keller, 1998; Vanselow and Keller, 2000), such that cytosolic  $\text{Ca}^{2+}$  loads are rapidly taken up into mitochondria, resulting in mitochondrial dysfunction and ROS generation (Carriedo et al., 2000; Rao et al., 2003). Based upon these observations, we have suggested that the high susceptibility of MNs to degeneration in disease may in part reflect a high propensity to oxidative stress. Whereas astrocyte dysfunction is a prominent feature in ALS and clearly contributes to the MN damage, its causes are poorly understood. In light of our findings that excitotoxic MN activation causes strong mitochondrial ROS generation, and the documented susceptibility of glutamate transport to oxidative disruption, we considered, and found evidence in support of, an hypothesis that ROS generated in MNs in response to Ca-AMPA receptor activation can contribute to oxidative dysfunction in surrounding astrocytes (Rao and Weiss, 2004; Rao et al., 2003), possibly contributing to the increased 3-NT labeling and the loss of GLT-1 labeling surrounding MNs we observed in G93A rats (Yin et al., 2007).

Another prominent feature of ALS is neuroinflammation, manifesting both cellular and humoral responses (Philips and Robberecht, 2011; Zhao et al., 2013). Activation of both astrocytes and microglia occur prominently, and activated microglia invade and contribute to phagocytosis of damaged MNs. The neuroinflammation also results in production of cytokines, which also can contribute to the MN damage. Of note the potent cytokine TNF- $\alpha$  can act on MNs to increase numbers of cell surface Ca-AMPA receptors, and thus their susceptibility to excitotoxic injury (Ferguson et al., 2008; Yin and Weiss, 2012), possibly accelerating the injury cascade. It is intriguing that BMAA infusions appear to reproduce astrocytic and microglial involvement resembling that seen in the SOD1 mutant rodent models. The mechanisms of this are uncertain, but in addition to the possibility discussed above that MN ROS generation contributes to astrocyte activation, MN damage may release antigens that contribute to the triggering of inflammatory responses. It is also possible that BMAA can induce effects directly on astrocytes, via a number of possible receptor dependent or independent mechanisms as discussed further below.

A distinct mechanism that is strongly suspected of contributing to MN degeneration in ALS concerns the accumulation of cytosolic protein aggregates (Blokhuys et al., 2013), reflecting an increased propensity for aggregate production in MNs, or defects in the ability to clear aggregates. In line with this idea, cytosolic protein aggregates are seen in all forms of ALS (with cytosolic TDP-43 aggregates specifically seen in most forms whether or not associated with mutations in the TDP-43 gene). Oxidative stress, as we suggest may occur prominently in MNs in response to excitotoxic  $\text{Ca}^{2+}$  loads, could promote protein misfolding and aggregate formation. Conversely, a family of ALS associated genes has been recently uncovered all of which normally function in protein degradative and autophagic pathways (Fecto and Siddique, 2011), suggesting that deficiencies in ability to get rid of aggregated

proteins and/or dysfunctional organelles (including mitochondria) could also be important contributors to disease. An important intracellular target of protein aggregates may be mitochondria, dysfunction in which is seen in all forms of ALS, and in particular mutant SOD1 aggregates are clearly documented to associate with and contribute to dysfunction of mitochondria (Manfredi and Xu, 2005).

### Clues to mechanisms of BMAA neurotoxicity

A number of studies of BMAA, mainly carried out using *in vitro* systems, have highlighted mechanisms through which BMAA may mediate neurotoxicity (Chiu et al., 2011; Vyas and Weiss, 2009). BMAA is an atypical non-protein amino acid. The first indication that it might act through excitotoxic mechanisms were provided by the observations that it could cause convulsions in rats (Polsky et al., 1972), and that it caused postsynaptic vacuolar changes in neurons similar to other excitotoxins (Nunn et al., 1987). Although early studies suggested that it caused excitotoxic tissue injury via weak activation of NMDA receptors (Kd ~ 1 mM in 1 day exposure) (Ross et al., 1987), it lacks the side-chain acidic or electronegative moiety characteristic of other excitatory amino acid compounds, having instead a positively charged amine group, leading to the suggestion the mechanism through which it activated glutamate receptors might be indirect (Nunn et al., 1987; Ross et al., 1987).

Providing a possible explanation for neuroexcitatory effects of BMAA, we found that BMAA could only activate glutamate receptors if bicarbonate was present in the extracellular buffer (Weiss and Choi, 1988). The presence of bicarbonate / CO<sub>2</sub> in the buffer results in the formation of carbamate adducts on the side chain amino groups (Myers and Nelson, 1990; Nunn and O'Brien, 1989), likely resulting in a structure resembling glutamate, in which the positively charged amine is replaced by an acidic group (Vyas and Weiss, 2009; Weiss et al., 1989a); and many subsequent studies have found evidence for excitotoxic effects of BMAA that are presumed to reflect the presence of the carbamate adduct; for a review see (Chiu et al., 2011).

A second question concerned the receptors through which BMAA mediates excitotoxic injury. Although BMAA is a weak agonist at NMDA receptors, we found that it caused selective degeneration of a subpopulation of cortical neurons ("NADPH-diaphorase" neurons) at far lower concentrations (30-100 μM) than needed for it to induce widespread damage via NMDA receptor activation, and that it mediated this selective injury via an AMPA rather than an NMDA receptor mechanism (Weiss et al., 1989b). Indeed, this finding, taken together with identification of 2 other environmental motor system toxins that acted through AMPA/kainate receptor mechanisms led us to undertake studies (discussed above) demonstrating the presence of Ca-AMPA receptors on MNs as a factor underlying an unusual susceptibility to AMPA receptor mediated injury (Carriedo et al., 1995; Carriedo et al., 1996; Van Den Bosch et al., 2000; Vandenberghe et al., 2000). We subsequently examined the vulnerability of MNs in dissociated spinal cord cultures to BMAA mediated neurotoxicity, and found that MNs were indeed selectively injured by BMAA, with 30-100 μM levels causing substantial MN degeneration over 24 hours, while mM levels were needed to cause widespread neuronal damage. Furthermore, the selective MN degeneration

was entirely blocked by the AMPA antagonist, NBQX, indicating that the MN degeneration was mediated through these receptors (Rao et al., 2006).

Other recent studies have highlighted additional ways in which BMAA might contribute to neurodegeneration. First, in addition to actions at NMDA and AMPA receptors described above, BMAA can activate metabotropic glutamate receptors (Copani et al., 1991). Intriguing recent studies suggest that micromolar levels of BMAA may be able to enhance diverse forms of neuronal injury (Lobner et al., 2007) through mechanisms including interference with function of the cysteine /glutamate antiporter (system Xc<sup>-</sup>) leading to glutathione depletion and increased oxidative stress, while promoting excess glutamate release (Liu et al., 2009). Metabolites of BMAA could also contribute to some of its effects (Nunn and Ponnusamy, 2009).

Another important issue concerns the ability of BMAA to get across the blood brain barrier and into the central nervous system (CNS), and its possible interactions with or incorporation into proteins, accounting for its apparent persistence in the CNS. As discussed above, BMAA has been isolated from tissues many years after the times of likely exposure, and levels recovered are greatly increased after acid hydrolysis, suggesting either incorporation or close association with proteins. Although early studies revealed that with systemic administration, some BMAA passes the blood brain barrier and enters the brain (Kisby et al., 1988) and that with repeated large oral dosage, free BMAA levels in rat brain can reach levels in the 100's of micromolar (Duncan et al., 1991), a recent study in rats examining the time course of brain BMAA uptake shows free soluble BMAA to appear first in the brain, with protein bound BMAA starting to accumulate within hours of administration, possibly consistent with its incorporation (Xie et al., 2013). An *in vitro* study recently found evidence for BMAA incorporation into proteins in place of L-serine (Dunlop et al., 2013), providing support for the hypothesis that incorporation could underlie the apparent long residence of BMAA in tissue protein fractions. Indeed, whatever the precise mechanism, long lasting association of BMAA with proteins may be critical to its apparent bioaccumulation in the food web, and provides a basis for BMAA to act as a slow neurotoxin, mediating toxicity for prolonged periods after the time of exposure, and accounting for the likely long latency between exposures and any occurrence of neurodegenerative disease. This slow toxicity could potentially reflect effects on proteins themselves as well as effects of free BMAA, which may be slowly released from the protein reservoir upon protein turnover.

## Conclusions

It is interesting and somewhat surprising that intrathecal infusions of BMAA can induce a pathological picture in spinal cord that in a number of ways – both involving degenerative changes in the MNs themselves, and changes in the neuropil and astrocytes in the ventral horn region surrounding the MNs – resembles that seen in the G93A mutant SOD1 overexpressing rat model as well as in diverse forms of human ALS. Indeed, it is notable that most human ALS shows a distinctive pathological phenotype despite the growing number of unrelated genes from distinct gene families that have been associated with genetic forms of the disease – suggesting that the characteristic pathological “picture” of ALS

results in large part from intrinsic features of MNs and their interdependencies with associated cells and environmental factors. Thus, in the case of BMAA induced pathological changes, the “picture” most likely reflects a combination of toxic mechanisms of BMAA superimposed upon the predisposition of the affected tissues.

As discussed above, prior studies have highlighted a number of ways in which BMAA is likely to promote pathophysiologically relevant mechanisms of MN degeneration. First, as we have found in culture models, exposures in the 10’s of  $\mu\text{M}$  range can trigger relatively selective MN injury via activation of Ca-AMPA receptors which are strongly expressed on MNs. In addition to directly damaging MNs, such excitotoxic activation of MNs by BMAA could, via mechanisms including induction of oxidative stress, contribute to the dysfunction of surrounding astrocytes. Although steady state levels of BMAA in the lumbar spinal fluid during present intrathecal infusions are unknown, the osmotic pump used releases  $\sim 0.25 \mu\text{l/hr}$  of 5 mM BMAA, which, if distributed in a local spinal CSF volume of  $\sim 250 \mu\text{l}$  (dilution of 1:1000/hr), and with a several hour half-life for CSF turnover, might yield steady state BMAA levels in the  $\sim 10\text{--}30 \mu\text{M}$ , which *in vitro* studies have suggested may well cause slow preferential MN damage. In addition, suggestions that BMAA may be misincorporated into or otherwise stably associated with proteins provides a potentially attractive mechanism to explain the long residence of BMAA in tissues and latency after exposure before disease onset, while possibly promoting protein misfolding and aggregation, as occurs in and has been considered likely to play pathogenic roles in neurodegenerative diseases including ALS (Blokhuis et al., 2013).

In sum, it is apparent that there is a wide spectrum of causes of ALS, with a number of clearly genetic causes triggered by mutations in distinct and unrelated genes from different gene families, as well as strong evidence for environmental contributions to the disease. In light of recent findings that BMAA is widespread in the environment, appears to be present in tissues of some human disease patients, and can contribute to the induction of a characteristic pathological phenotype (as seen here), likely acting through mechanisms (excitotoxicity, oxidative stress, protein misfolding) that are known to occur in ALS, might BMAA be an important toxin of interest to the disease meriting further investigation (Bradley et al., 2013)?

## Acknowledgments

This work was supported by NIH grant NS36548 (JHW), and a grant from the Muscular Dystrophy Association (JHW).

## Abbreviations

(AMPA)	$\alpha$ -amino-3-hydroxy-5-methyl-4-isoxazolepropionic acid
(ALS)	amyotrophic lateral sclerosis
(ALS/PDC)	amyotrophic lateral sclerosis–Parkinsonism Dementia Complex of Guam
(BMAA)	beta-N-methylamino-L-alanine

<b>(Ca-AMPA receptors)</b>	Ca <sup>2+</sup> permeable AMPA receptors
<b>(GLT-1)</b>	glutamate transporter 1
<b>(MN)</b>	motor neuron
<b>(SOD1)</b>	superoxide dismutase type 1
<b>(TDP-43)</b>	TAR DNA-binding protein 43

## References

- Alexianu ME, Ho BK, Mohamed AH, La Bella V, Smith RG, Appel SH. The role of calcium-binding proteins in selective motoneuron vulnerability in amyotrophic lateral sclerosis. *Ann Neurol.* 1994; 36:846–858. [PubMed: 7998770]
- Arnold A, D.C. E. V.S. P. Amyotrophic Lateral Sclerosis; Fifty Cases observed on Guam. *J Nerve Ment Dis.* 1953:135–139.
- Beal MF, Ferrante RJ, Browne SE, Matthews RT, Kowall NW, Brown RH Jr. Increased 3-nitrotyrosine in both sporadic and familial amyotrophic lateral sclerosis. *Ann Neurol.* 1997; 42:644–654. [PubMed: 9382477]
- Blokhuis AM, Groen EJ, Koppers M, van den Berg LH, Pasterkamp RJ. Protein aggregation in amyotrophic lateral sclerosis. *Acta neuropathologica.* 2013; 125:777–794. [PubMed: 23673820]
- Bradley WG, Borenstein AR, Nelson LM, Codd GA, Rosen BH, Stommel EW, Cox PA. Is exposure to cyanobacteria an environmental risk factor for amyotrophic lateral sclerosis and other neurodegenerative diseases? *Amyotrophic lateral sclerosis & frontotemporal degeneration.* 2013; 14:325–333. [PubMed: 23286757]
- Brand LE, Pablo J, Compton A, Hammerschlag N, Mash DC. Cyanobacterial Blooms and the Occurrence of the neurotoxin beta-N-methylamino-L-alanine (BMAA) in South Florida Aquatic Food Webs. *Harmful algae.* 2010; 9:620–635. [PubMed: 21057660]
- Carriedo SG, Sensi SL, Yin HZ, Weiss JH. AMPA exposures induce mitochondrial Ca(2+) overload and ROS generation in spinal motor neurons in vitro. *J Neurosci.* 2000; 20:240–250. [PubMed: 10627601]
- Carriedo SG, Yin HZ, Lamberta R, Weiss JH. In vitro kainate injury to large, SMI-32(+) spinal neurons is Ca<sup>2+</sup> dependent. *Neuroreport.* 1995; 6:945–948. [PubMed: 7612889]
- Carriedo SG, Yin HZ, Weiss JH. Motor neurons are selectively vulnerable to AMPA/kainate receptor-mediated injury in vitro. *J Neurosci.* 1996; 16:4069–4079. [PubMed: 8753869]
- Chiu AS, Gehringer MM, Welch JH, Neilan BA. Does alpha-amino-beta-methylaminopropionic acid (BMAA) play a role in neurodegeneration? *International journal of environmental research and public health.* 2011; 8:3728–3746. [PubMed: 22016712]
- Copani A, Canonico PL, Catania MV, Aronica E, Bruno V, Ratti E, van Amsterdam FT, Gaviraghi G, Nicoletti F. Interaction between beta-N-methylamino-L-alanine and excitatory amino acid receptors in brain slices and neuronal cultures. *Brain Res.* 1991; 558:79–86. [PubMed: 1657313]
- Cox PA, Banack SA, Murch SJ. Biomagnification of cyanobacterial neurotoxins and neurodegenerative disease among the Chamorro people of Guam. *Proc Natl Acad Sci U S A.* 2003; 100:13380–13383. [PubMed: 14612559]
- Cox PA, Banack SA, Murch SJ, Rasmussen U, Tien G, Bidigare RR, Metcalf JS, Morrison LF, Codd GA, Bergman B. Diverse taxa of cyanobacteria produce beta-N-methylamino-L-alanine, a neurotoxic amino acid. *Proc Natl Acad Sci U S A.* 2005; 102:5074–5078. [PubMed: 15809446]
- Duncan MW, Steele JC, Kopin IJ, Markey SP. 2-Amino-3-(methylamino)-propanoic acid (BMAA) in cycad flour: an unlikely cause of amyotrophic lateral sclerosis and parkinsonism/dementia of Guam. *Neurology.* 1990; 40:767–772. [PubMed: 2330104]
- Duncan MW, Villacreses NE, Pearson PG, Wyatt L, Rapoport SI, Kopin IJ, Markey SP, Smith QR. 2-amino-3-(methylamino)-propanoic acid (BMAA) pharmacokinetics and blood-brain barrier permeability in the rat. *J Pharmacol Exp Ther.* 1991; 258:27–35. [PubMed: 2072299]

- Dunlop RA, Cox PA, Banack SA, Rodgers KJ. The Non-Protein Amino Acid BMAA Is Misincorporated into Human Proteins in Place of l-Serine Causing Protein Misfolding and Aggregation. 8. *PLoS One*. 2013; 8:e75376. [PubMed: 24086518]
- Elliott JL, Snider WD. Parvalbumin is a marker of ALS-resistant motor neurons. *Neuroreport*. 1995; 6:449–452. [PubMed: 7766841]
- Fecto F, Siddique T. Making connections: pathology and genetics link amyotrophic lateral sclerosis with frontotemporal lobe dementia. *Journal of molecular neuroscience : MN*. 2011; 45:663–675. [PubMed: 21901496]
- Ferguson AR, Christensen RN, Gensel JC, Miller BA, Sun F, Beattie EC, Bresnahan JC, Beattie MS. Cell death after spinal cord injury is exacerbated by rapid TNF alpha-induced trafficking of GluR2-lacking AMPARs to the plasma membrane. *J Neurosci*. 2008; 28:11391–11400. [PubMed: 18971481]
- Ferrante RJ, Shinobu LA, Schulz JB, Matthews RT, Thomas CE, Kowall NW, Gurney ME, Beal MF. Increased 3-nitrotyrosine and oxidative damage in mice with a human copper/zinc superoxide dismutase mutation. *Ann Neurol*. 1997; 42:326–334. [PubMed: 9307254]
- Garruto RM, Yase Y. Neurodegenerative disorders of the western pacific: the search for mechanisms of pathogenesis. *Trends in Neurosciences*. 1986; 9:368–374.
- Howland DS, Liu J, She Y, Goad B, Maragakis NJ, Kim B, Erickson J, Kulik J, DeVito L, Psaltis G, DeGennaro LJ, Cleveland DW, Rothstein JD. Focal loss of the glutamate transporter EAAT2 in a transgenic rat model of SOD1 mutant-mediated amyotrophic lateral sclerosis (ALS). *Proc Natl Acad Sci U S A*. 2002; 99:1604–1609. [PubMed: 11818550]
- Jonasson S, Eriksson J, Berntzon L, Spacil Z, Ilag LL, Ronnevi LO, Rasmussen U, Bergman B. Transfer of a cyanobacterial neurotoxin within a temperate aquatic ecosystem suggests pathways for human exposure. *Proc Natl Acad Sci U S A*. 2010; 107:9252–9257. [PubMed: 20439734]
- Karamyan VT, Speth RC. Animal models of BMAA neurotoxicity: a critical review. *Life Sci*. 2008; 82:233–246. [PubMed: 18191417]
- Kisby GE, Roy DN, Spencer PS. Determination of beta-N-methylamino-L-alanine (BMAA) in plant (*Cycas circinalis* L.) and animal tissue by precolumn derivatization with 9-fluorenylmethyl chloroformate (FMOC) and reversed-phase high-performance liquid chromatography. *J Neurosci Methods*. 1988; 26:45–54. [PubMed: 3199847]
- Koerner DR. Amyotrophic lateral sclerosis on Guam. *Annals of internal medicine*. 1952; 37:1204–1220. [PubMed: 13008298]
- Kurland LT. An appraisal of the neurotoxicity of cycad and the etiology of amyotrophic lateral sclerosis on Guam. *Fed Proc*. 1972; 31:1540–1542. [PubMed: 4561643]
- Lips MB, Keller BU. Endogenous calcium buffering in motoneurons of the nucleus hypoglossus from mouse. *J Physiol*. 1998; 511:105–117. [PubMed: 9679167]
- Liu X, Rush T, Zapata J, Lobner D. beta-N-methylamino-l-alanine induces oxidative stress and glutamate release through action on system Xc(-). *Exp Neurol*. 2009; 217:429–433. [PubMed: 19374900]
- Lobner D, Piana PM, Salous AK, Peoples RW. Beta-N-methylamino-L-alanine enhances neurotoxicity through multiple mechanisms. *Neurobiol Dis*. 2007; 25:360–366. [PubMed: 17098435]
- Manfredi G, Xu Z. Mitochondrial dysfunction and its role in motor neuron degeneration in ALS. *Mitochondrion*. 2005; 5:77–87. [PubMed: 16050975]
- Metcalf JS, Banack SA, Lindsay J, Morrison LF, Cox PA, Codd GA. Co-occurrence of beta-N-methylamino-L-alanine, a neurotoxic amino acid with other cyanobacterial toxins in British waterbodies, 1990-2004. *Environmental microbiology*. 2008; 10:702–708. [PubMed: 18237305]
- Mondo K, Hammerschlag N, Basile M, Pablo J, Banack SA, Mash DC. Cyanobacterial neurotoxin beta-N-methylamino-L-alanine (BMAA) in shark fins. *Marine drugs*. 2012; 10:509–520. [PubMed: 22412816]
- Mulder DW, T.K. K. Iriarte LL. Neurologic disease on the island of Guam. *U.S. Armed Forces Medical Journal*. 1954; 5:1724–1739.
- Murch SJ, Cox PA, Banack SA. A mechanism for slow release of biomagnified cyanobacterial neurotoxins and neurodegenerative disease in Guam. *Proc Natl Acad Sci U S A*. 2004a; 101:12228–12231. [PubMed: 15295100]

- Murch SJ, Cox PA, Banack SA, Steele JC, Sacks OW. Occurrence of beta-methylamino-l-alanine (BMAA) in ALS/PDC patients from Guam. *Acta neurologica Scandinavica*. 2004b; 110:267–269. [PubMed: 15355492]
- Myers TG, Nelson SD. Neuroactive carbamate adducts of beta-N-methylamino-L-alanine and ethylenediamine. Detection and quantitation under physiological conditions by <sup>13</sup>C NMR. *J Biol Chem*. 1990; 265:10193–10195. [PubMed: 2113048]
- Neumann M, Sampathu DM, Kwong LK, Truax AC, Micsenyi MC, Chou TT, Bruce J, Schuck T, Grossman M, Clark CM, McCluskey LF, Miller BL, Masliah E, Mackenzie IR, Feldman H, Feiden W, Kretzschmar HA, Trojanowski JQ, Lee VM. Ubiquitinated TDP-43 in frontotemporal lobar degeneration and amyotrophic lateral sclerosis. *Science*. 2006; 314:130–133. [PubMed: 17023659]
- Nunn PB, O'Brien P. The interaction of beta-N-methylamino-L-alanine with bicarbonate: an <sup>1</sup>H-NMR study. *FEBS Lett*. 1989; 251:31–35. [PubMed: 2666171]
- Nunn PB, Ponnusamy M. Beta-N-methylaminoalanine (BMAA): metabolism and metabolic effects in model systems and in neural and other tissues of the rat in vitro. *Toxicol : official journal of the International Society on Toxinology*. 2009; 54:85–94. [PubMed: 19285998]
- Nunn PB, Seelig M, Zagoren JC, Spencer PS. Stereospecific acute neuronotoxicity of 'uncommon' plant amino acids linked to human motor-system diseases. *Brain Res*. 1987; 410:375–379. [PubMed: 3109690]
- Pablo J, Banack SA, Cox PA, Johnson TE, Papapetropoulos S, Bradley WG, Buck A, Mash DC. Cyanobacterial neurotoxin BMAA in ALS and Alzheimer's disease. *Acta neurologica Scandinavica*. 2009; 120:216–225. [PubMed: 19254284]
- Philips T, Robberecht W. Neuroinflammation in amyotrophic lateral sclerosis: role of glial activation in motor neuron disease. *Lancet neurology*. 2011; 10:253–263.
- Polsky FI, Nunn PB, Bell EA. Distribution and toxicity of alpha-amino-beta-methylaminopropionic acid. *Fed Proc*. 1972; 31:1473–1475. [PubMed: 5056173]
- Rao SD, Banack SA, Cox PA, Weiss JH. BMAA selectively injures motor neurons via AMPA/kainate receptor activation. *Exp Neurol*. 2006; 201:244–252. [PubMed: 16764863]
- Rao SD, Weiss JH. Excitotoxic and oxidative cross-talk between motor neurons and glia in ALS pathogenesis. *Trends Neurosci*. 2004; 27:17–23. [PubMed: 14698606]
- Rao SD, Yin HZ, Weiss JH. Disruption of glial glutamate transport by reactive oxygen species produced in motor neurons. *J Neurosci*. 2003; 23:2627–2633. [PubMed: 12684448]
- Robertson J, Sanelli T, Xiao S, Yang W, Horne P, Hammond R, Piro EP, Strong MJ. Lack of TDP-43 abnormalities in mutant SOD1 transgenic mice shows disparity with ALS. *Neurosci Lett*. 2007; 420:128–132. [PubMed: 17543992]
- Ross SM, Seelig M, Spencer PS. Specific antagonism of excitotoxic action of 'uncommon' amino acids assayed in organotypic mouse cortical cultures. *Brain Res*. 1987; 425:120–127. [PubMed: 3123008]
- Rothstein JD, Martin LJ, Kuncl RW. Decreased glutamate transport by the brain and spinal cord in amyotrophic lateral sclerosis. *N Engl J Med*. 1992; 326:1464–1468. [PubMed: 1349424]
- Rothstein JD, Van Kammen M, Levey AI, Martin LJ, Kuncl RW. Selective loss of glial glutamate transporter GLT-1 in amyotrophic lateral sclerosis. *Ann Neurol*. 1995; 38:73–84. [PubMed: 7611729]
- Roy J, Minotti S, Dong L, Figlewicz DA, Durham HD. Glutamate potentiates the toxicity of mutant Cu/Zn-superoxide dismutase in motor neurons by postsynaptic calcium-dependent mechanisms. *J Neurosci*. 1998; 18:9673–9684. [PubMed: 9822728]
- Shan X, Vocadlo D, Krieger C. Mislocalization of TDP-43 in the G93A mutant SOD1 transgenic mouse model of ALS. *Neurosci Lett*. 2009; 458:70–74. [PubMed: 19379791]
- Spencer PS. Guam ALS/parkinsonism-dementia: a long-latency neurotoxic disorder caused by "slow toxin(s)" in food? *Can J Neurol Sci*. 1987; 14:347–357. [PubMed: 3315142]
- Spencer PS, Nunn PB, Hugon J, Ludolph AC, Ross SM, Roy DN, Robertson RC. Guam amyotrophic lateral sclerosis-parkinsonism-dementia linked to a plant excitant neurotoxin. *Science*. 1987; 237:517–522. [PubMed: 3603037]

- Turner BJ, Baumer D, Parkinson NJ, Scaber J, Ansorge O, Talbot K. TDP-43 expression in mouse models of amyotrophic lateral sclerosis and spinal muscular atrophy. *BMC neuroscience*. 2008; 9:104. [PubMed: 18957104]
- Van Den Bosch L, Vandenberghe W, Klaassen H, Van Houtte E, Robberecht W. Ca(2+)-permeable AMPA receptors and selective vulnerability of motor neurons. *J Neurol Sci*. 2000; 180:29–34. [PubMed: 11090861]
- Vandenberghe W, Robberecht W, Brorson JR. AMPA receptor calcium permeability, GluR2 expression, and selective motoneuron vulnerability. *J Neurosci*. 2000; 20:123–132. [PubMed: 10627588]
- Vanselow BK, Keller BU. Calcium dynamics and buffering in oculomotor neurones from mouse that are particularly resistant during amyotrophic lateral sclerosis (ALS)- related motoneurone disease. *J Physiol*. 2000; 525(Pt 2):433–445. [PubMed: 10835045]
- Vega A, Bell EA. Alpha-amino-beta-methylaminopropanoic acid, a new amino acid from seeds of *cycas circinalis*. *Phytochem*. 1967; 6:759–762.
- Vyas KJ, Weiss JH. BMAA--an unusual cyanobacterial neurotoxin. Amyotrophic lateral sclerosis : official publication of the World Federation of Neurology Research Group on Motor Neuron Diseases. 2009; 10(Suppl 2):50–55.
- Weiss JH, Choi DW. Beta-N-methylamino-L-alanine neurotoxicity: requirement for bicarbonate as a cofactor. *Science*. 1988; 241:973–975. [PubMed: 3136549]
- Weiss JH, Christine CW, Choi DW. Bicarbonate dependence of glutamate receptor activation by beta-N-methylamino-L-alanine: channel recording and study with related compounds. *Neuron*. 1989a; 3:321–326. [PubMed: 2561969]
- Weiss JH, Koh JY, Choi DW. Neurotoxicity of beta-N-methylamino-L-alanine (BMAA) and beta-N-oxallylamino-L-alanine (BOAA) on cultured cortical neurons. *Brain Res*. 1989b; 497:64–71. [PubMed: 2551452]
- Whiting MG. Toxicity of Cycads. *Economic Botany*. 1963; 17:271–302.
- Xie X, Basile M, Mash DC. Cerebral uptake and protein incorporation of cyanobacterial toxin beta-N-methylamino-L-alanine. *Neuroreport*. 2013; 24:779–784. [PubMed: 23979257]
- Yin HZ, Tang DT, Weiss JH. Intrathecal infusion of a Ca(2+)-permeable AMPA channel blocker slows loss of both motor neurons and of the astrocyte glutamate transporter, GLT-1 in a mutant SOD1 rat model of ALS. *Exp Neurol*. 2007; 207:177–185. [PubMed: 17719032]
- Yin HZ, Weiss JH. Marked synergism between mutant SOD1 and glutamate transport inhibition in the induction of motor neuronal degeneration in spinal cord slice cultures. *Brain Res*. 2012; 1448:153–162. [PubMed: 22370146]
- Zhao W, Beers DR, Appel SH. Immune-mediated mechanisms in the pathoprogession of amyotrophic lateral sclerosis. *Journal of neuroimmune pharmacology : the official journal of the Society on NeuroImmune Pharmacology*. 2013; 8:888–899. [PubMed: 23881705]



### Highlights

- Prolonged intrathecal infusions of BMAA were carried out in WT and SOD1 mutant rats
- Pathological changes induced by BMAA were similar to those induced by mutant SOD1
- Changes were selectively observed in ventral horn with minimal dorsal horn changes
- Changes included MNs in different stages of degeneration with surrounding astrogliosis
- Findings may be compatible with contributions of BMAA in some human ALS

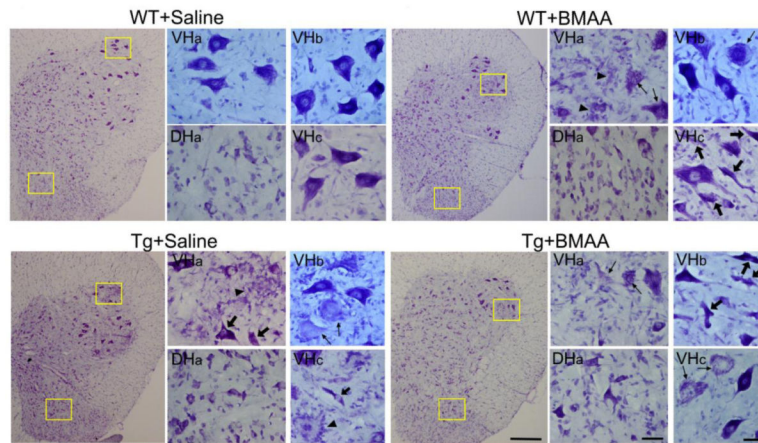


**Figure 1. Thirty day BMAA infusions induce a similar spectrum of morphological changes in rat ventral horn MNs as is seen in presymptomatic rats harboring the G93A SOD1 mutation**  
 G93A SOD1 mutant rats and sibling WT rats were subjected to 30 day intrathecal infusions of BMAA or saline (from  $80 \pm 2$  to  $110 \pm 2$  days of age) as described, followed by perfusion, sectioning of the lumbar spinal cords and Nissl staining to examine cellular morphology. For each treatment (as indicated), a low power image of a representative hemi-section of the lumbar spinal cord (40x) is shown, and details (VHa and DHa) show high power (400x) views of the marked regions of the ventral horn and the dorsal horn respectively. VHb and VHa show other representative high power views of ventral horn sections from the same treatment. In contrast to the healthy appearing MNs in the WT+saline condition, MNs in the Tg+saline condition displayed a spectrum of degenerative morphologies including cell swelling and vacuolar changes (thin arrows), MN shrinkage (thick arrows), and microglial infiltration or glial nodule formation (arrowheads). A similar spectrum of changes was noted in the WT+BMAA and Tg+BMAA conditions. In contrast to the marked changes noted in ventral horn MNs, little evidence of dorsal horn neuronal damage was noted in any of the conditions. Scale bar = 400  $\mu$ m (low power panels) or 50  $\mu$ m (all other panels).

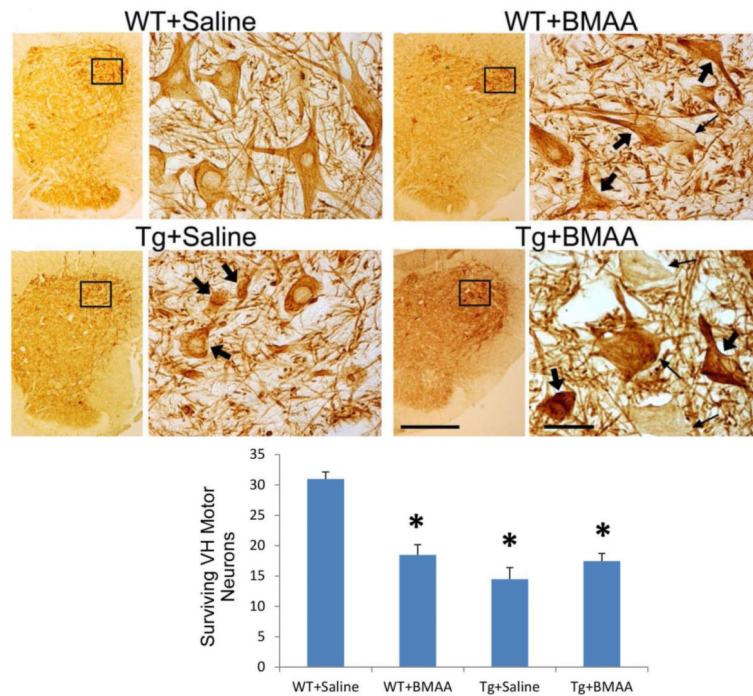


**Figure 2. Morphological changes and quantification of lumbar ventral horn MN degeneration induced by the G93A SOD1 mutation and by 30 day BMAA infusions**

G93A mutant SOD1 and sibling WT rats were subjected to 30 day intrathecal infusions with BMAA or saline as described, followed by perfusion, sectioning of the lumbar spinal cords and SMI-32 immunostaining for counts of surviving MNs. SMI-32 labeling provides excellent visualization of somatic and dendritic morphology and is thus useful for assessing structural damage.

**TOP: Morphological changes.** For each treatment (as indicated), a low power image of a representative SMI-32 stained hemi-section of the lumbar spinal cord (40x) is shown, along with a high power (400x) view of the marked region of ventral horn. As in Figure 1, above, note the intact somatic and dendritic morphology in the control condition (WT+saline), and the mix of somatic changes with some MNs showing atrophy (thick arrows) and some showing swelling (thin arrows), as well as widespread fragmentation of dendritic processes in the other conditions. Scale bar = 500  $\mu$ m (low power panels) or 50  $\mu$ m (all other panels).

**BOTTOM: Quantification of MNs cell loss.** Healthy appearing intact MNs were counted in SMI-32 immunostained slices from each condition. Values represent mean number of intact ventral horn MNs per section (comprising two ventral horns), as assessed by direct microscopic examination. Each data point reflects the mean value from 5-9 animals (WT +BMAA, 9; WT+saline, 6; Tg+saline, 5; Tg+BMAA, 5 animals); all ventral horn MNs were counted in each of 18-23 slices from each animal, with a total of 1700-3500 MNs counted in each condition. \*indicates difference from WT animals by two tailed t-test ( $p < 0.001$ ).

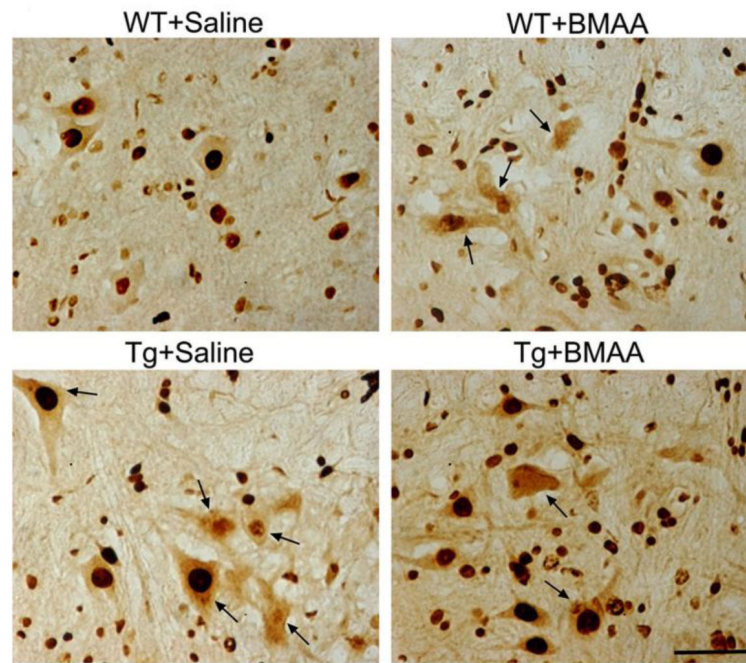


**Figure 3. The G93A SOD1 mutation and 30 day BMAA infusions both induce the appearance of cytosolic TDP-43 immunoreactive aggregates in some MNs**

G93A mutant SOD1 and sibling WT rats were subjected to 30 day intrathecal infusions with BMAA or saline as described, followed by perfusion, sectioning of the lumbar spinal cords and immunostaining for TDP-43. Note that the TDP-43 labeling in large MNs is distinctly nuclear in the WT+saline condition, whereas in the other conditions, some of the large MNs (indicated by arrows) show disruption of homogeneous nuclear labeling and accumulation of cytosolic aggregates. Scale bar = 100  $\mu$ m.

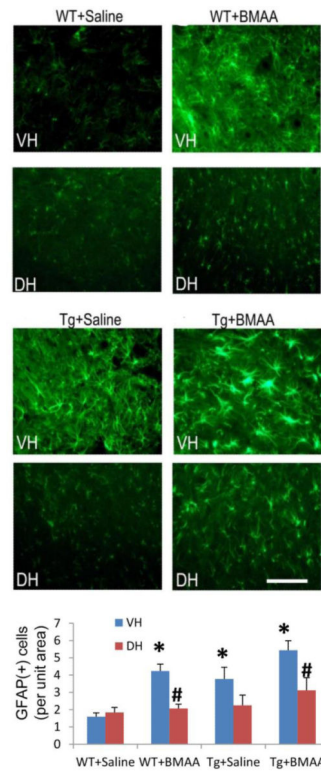


**Figure 4. The G93A SOD1 mutation and 30 day BMAA infusions both induce prominent reactive astrogliosis in the ventral horn**

G93A mutant SOD1 and sibling WT rats were subjected to 30 day intrathecal infusions with BMAA or saline as described, followed by perfusion, sectioning of the lumbar spinal cords and immunostaining for GFAP.

**TOP:** For each treatment (as indicated), images show representative high power (200x) immunofluorescence views from ventral horn (VH) and dorsal horn (DH) regions of the spinal cord gray matter. Note that compared to the control (WT+saline) condition, all of the other conditions show a marked increase in number and intensity of GFAP labeled reactive astrocytes in the ventral horn. Further note that GFAP labeling is not increased in the dorsal horn, with the possible exception of the Tg+BMAA condition, in which there appeared to be a slight increase in GFAP labeling. Scale bar=100  $\mu$ m.

**BOTTOM:** Quantification of GFAP labeling. Reactive astrocytes were counted in GFAP immunolabeled slices from each condition. Values represent mean number of distinct GFAP-positive astrocytes per unit area in 200x microscope fields. Each data point represents the mean value from 5 to 8 animals; for each animal all GFAP immunoreactive astrocytes were counted in each of 6 ventral horn and dorsal horn sections (with ~ 500-1500 cells counted for each condition). \* indicates difference from VH in WT+saline condition ( $p < 0.02$ ); # indicated difference from VH in the same condition ( $p < 0.05$ ) by two-tailed t test.

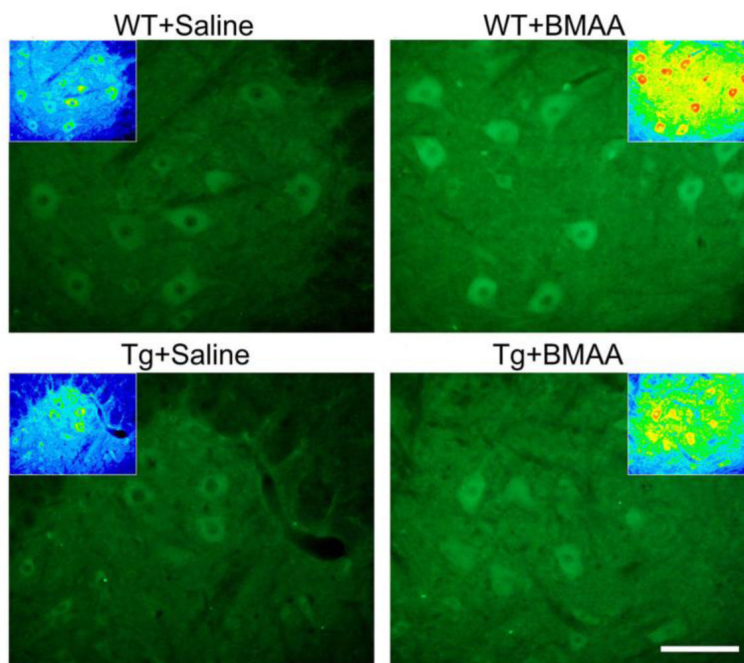


**Figure 5. Effects of the G93A SOD1 mutation and of 30 day BMAA infusions on 3-NT labeling in ventral horn**

G93A mutant SOD1 and sibling WT rats were subjected to 30 day intrathecal infusions with BMAA or saline as described, followed by perfusion, sectioning of the lumbar spinal cords and immunostaining for 3-NT. For each treatment (as indicated), images show representative high power (200x) immunofluorescence views from 3-NT immunolabeled slices. Inserts show the same regions displayed using pseudocolor (8 bit) representations of fluorescence, in order to highlight the gradient in labeling intensity. Note the moderate labeling of WT MNs, and the clear increased labeling in the WT+BMAA and Tg+BMAA conditions not only in the MNs, but prominently in the neuropil surrounding and between MNs. Scale bar = 100  $\mu$ m.

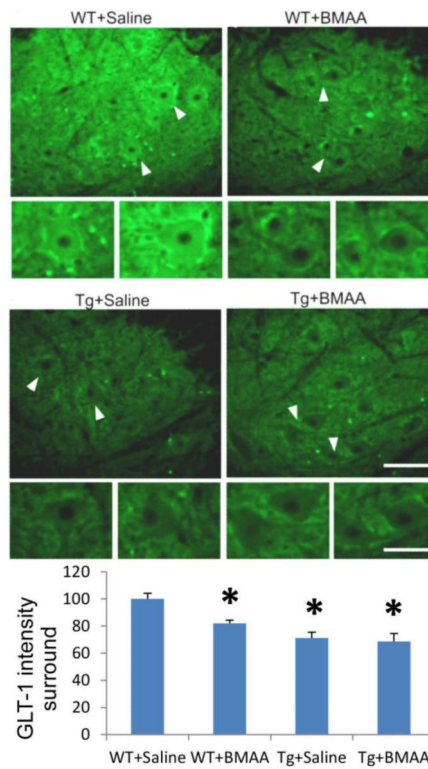


**Figure 6. The G93A SOD1 mutation and 30 day BMAA infusions each induce loss of the astrocytic glutamate transporter, GLT-1, in regions surrounding ventral horn astrocytes**  
G93A mutant SOD1 and sibling WT rats were subjected to 30 day intrathecal infusions with BMAA or saline as described, followed by perfusion, sectioning of the lumbar spinal cords and immunostaining for GLT-1.

**TOP:** For each treatment (as indicated), images show representative 200x immunofluorescence views from GLT-1 immunolabeled slices; details show blow-ups of the regions marked by arrowheads. Note the strong GLT-1 labeling often seen immediately surrounding ventral horn MNs in the WT+saline condition, in contrast to the marked loss of GLT-1 labeling surrounding ventral horn MNs in the other conditions. Scale bar = 100  $\mu$ m (low power), 50  $\mu$ m (high power images),

**BOTTOM:** Quantification of GLT-1 labeling intensity in 10  $\mu$ m wide zones surrounding MN somata. Values represent the mean fluorescence compared to control (WT+saline =100%) in the surround regions from 5-9 animals for each condition, based on measurements from 10-12 ventral horns sections per animal and a total of 500-1000 MN surrounds measurements in each conditions. \* indicates difference from WT+saline by two-tailed t test ( $p < 0.002$ ).